

# Developing an Immunocompetent Mouse Lung Cancer Model for the Evaluation of Virotherapy Effectiveness

Eric Riedinger<sup>1</sup>, Jonathan Nitz<sup>1</sup>, Kelly M. McMasters<sup>1,2</sup>, and Jorge G. Gomez-Gutierrez<sup>1</sup>

<sup>1</sup>The Hiram C. Polk MD Department of Surgery and <sup>2</sup>James Graham Brown Cancer Center, University of Louisville, School of Medicine, Louisville, KY, 40202.

## Introduction

The preclinical characterization of oncolytic adenoviruses has so far been restricted to immunodeficient xenograft tumor models because human adenoviruses do not replicate efficiently in murine tumor cells.

These immunodeficient animal models can demonstrate effective replication in and destruction of human tumors by adenovirus type 5 (Ad5)-based vectors. However, the viruses do not replicate in mouse tissues, and thus the models can neither assess the complete safety and efficacy profile of the vectors in normal tissue, nor do they permit evaluation of the impact of an active immune system on overall vector potency. In contrast, the effect of virus replication and the immune response could be evaluated in an immunocompetent syngeneic tumor model.

Previously it has been reported that autophagy plays a key role in oncolytic adenovirus replication. Moreover, the chemotherapeutic agent Temozolomide (TMZ), an autophagy inducer, enhances virotherapy effectiveness in human glioblastoma cells. We hypothesize that TMZ-induced autophagy will enhance oncolytic Ad replication in mouse Lewis Lung Carcinoma-1 (LLC-1) thereby enhancing cancer cell killing effect. This study evaluated the ability of TMZ to enhance oncolytic Ad replication in the syngeneic mouse C57BL LLC-1 cell line.

## Results

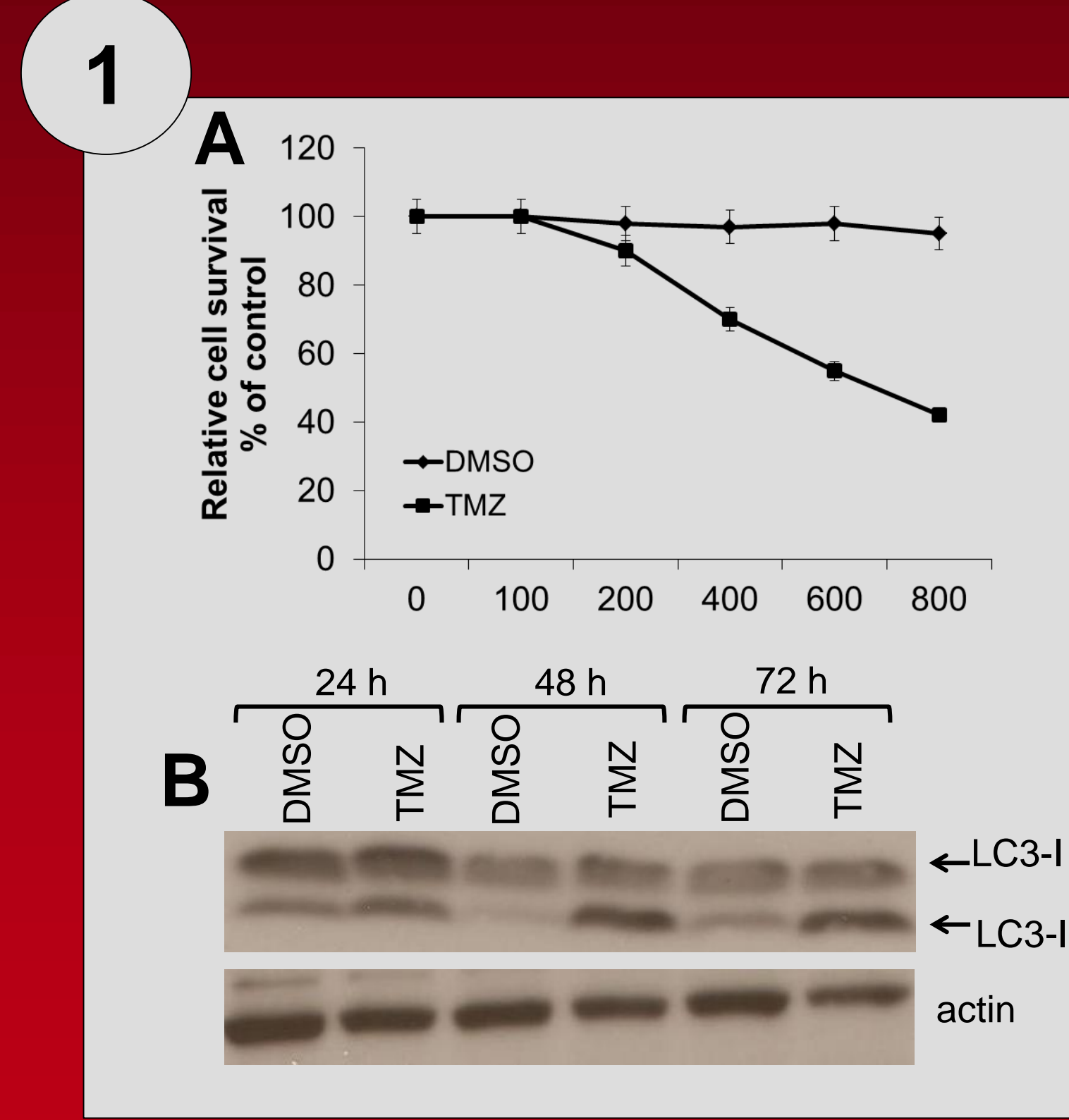


Fig. 1. **A)** MTT assay to evaluate the TMZ cytotoxic effect in LLC-1 cells. **B)** WB to assess the autophagy induction in LLC-1 treated with TMZ.

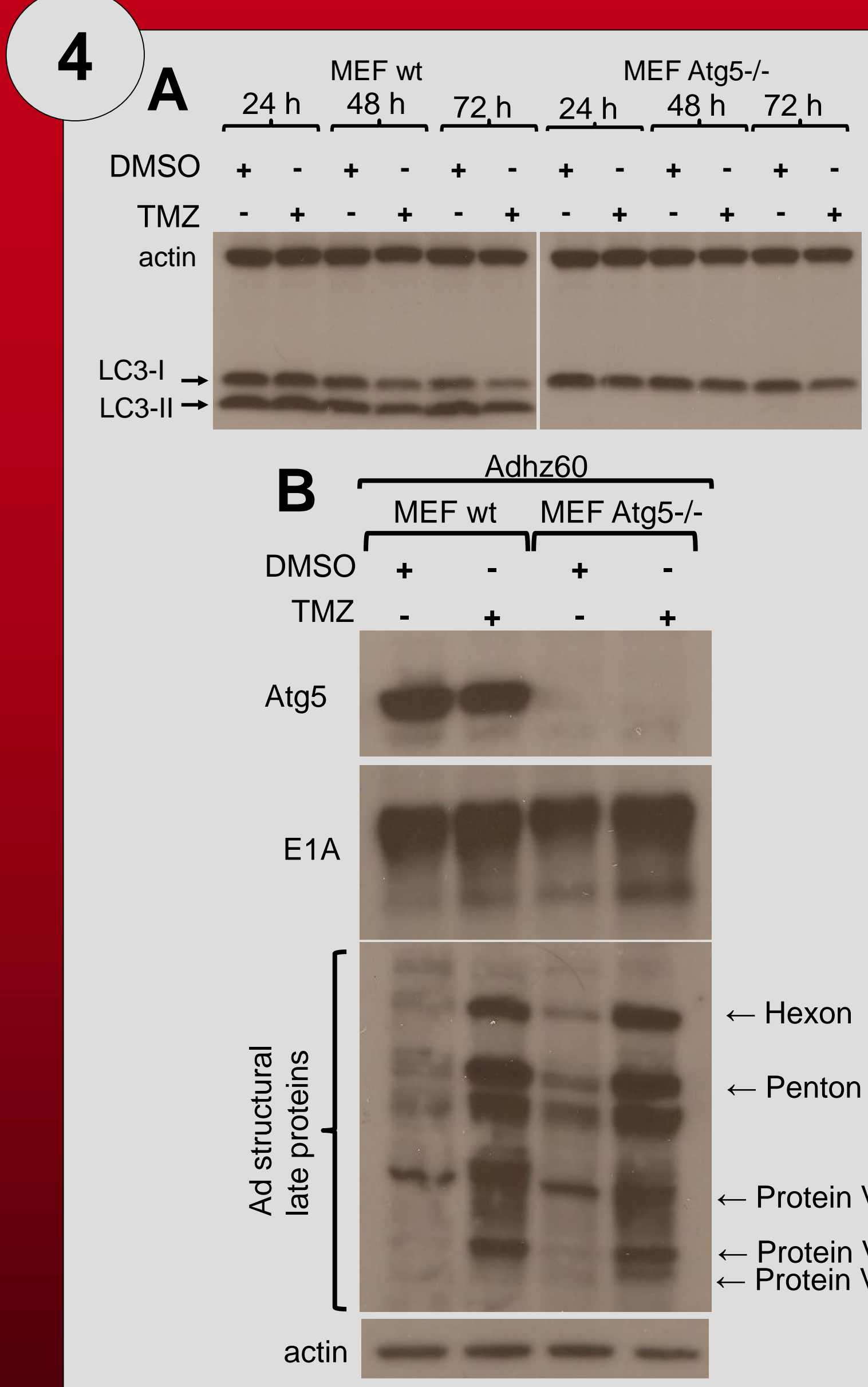


Fig. 4. **A)** Evaluation of LC3-II expression in MEF wt and Atg-5 knockout cells treated with TMZ. **B)** Evaluation of Ad E1A and late proteins expression.

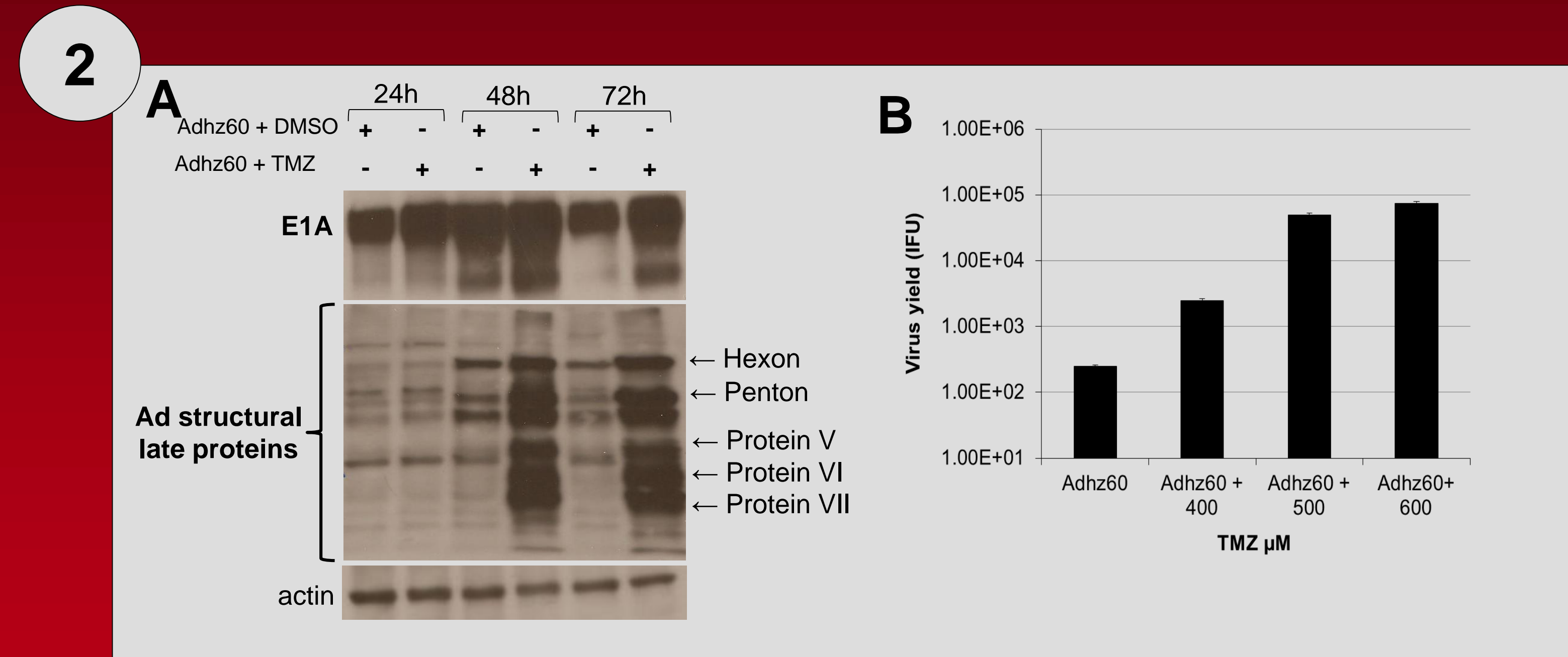


Fig. 2. **A)** Temozolomide enhances oncolytic Ad early and structural late proteins expression in mouse LLC-1 cells. **B)** Mouse Lewis Lung Carcinoma-1 cells are able to support oncolytic adenovirus replication upon treatment with TMZ.

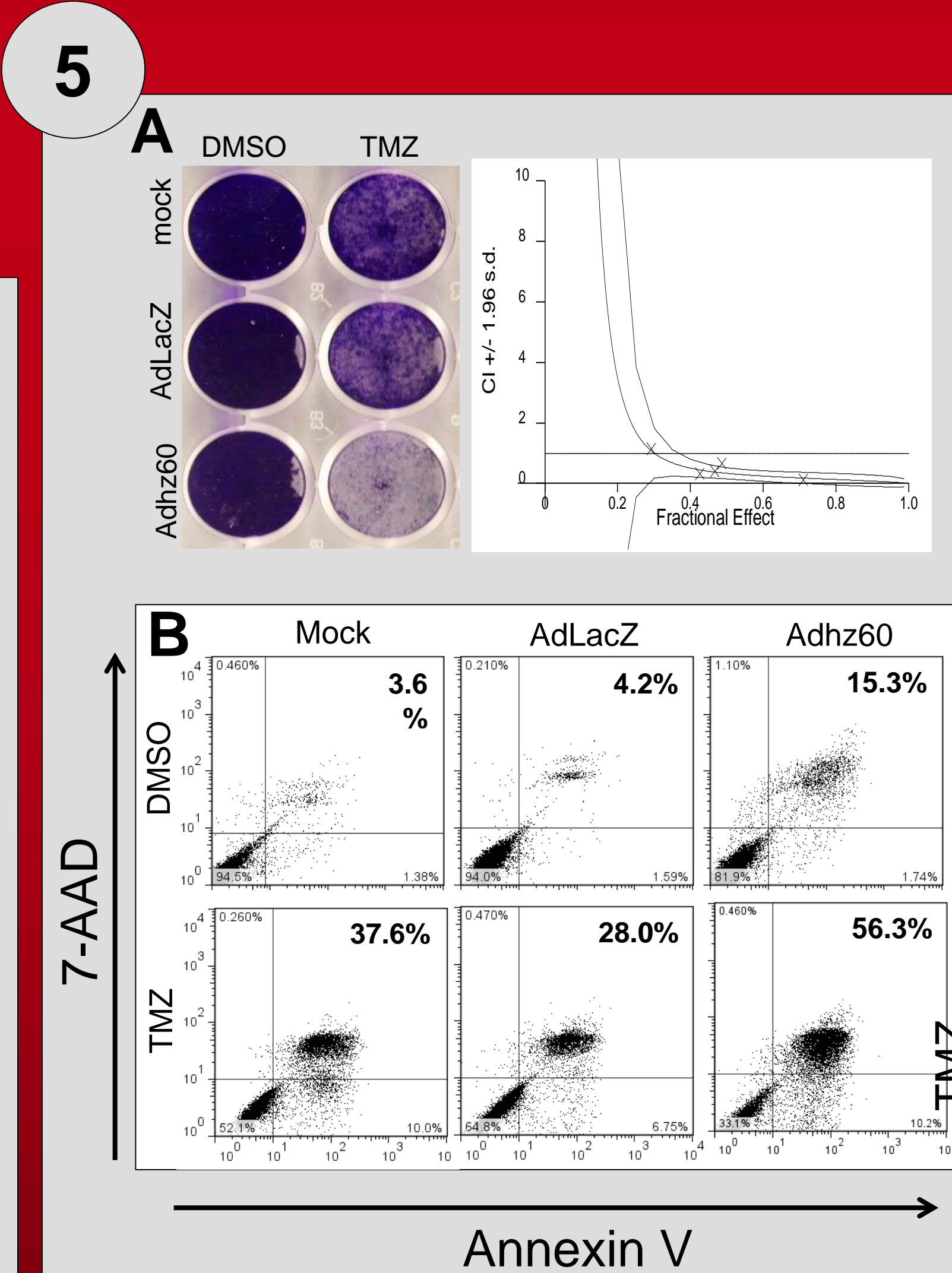


Fig. 5. **A)** Combination therapy of oncolytic adenovirus and TMZ has a synergistic cancer killing affect and **B)** Apoptosis induction.

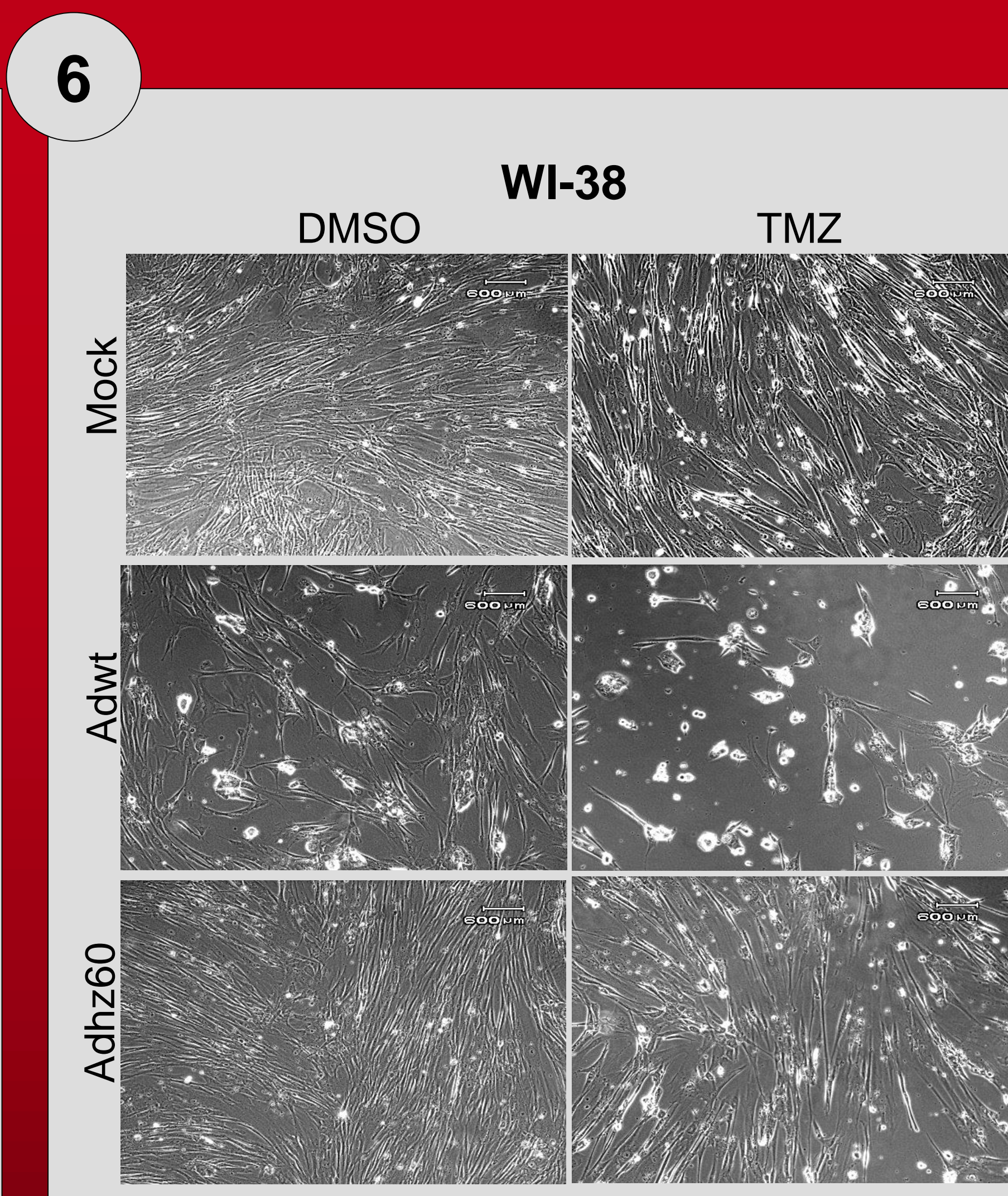


Fig. 6. Combination therapy of oncolytic adenovirus and TMZ induces minimum cytopathic effect in human lung normal cells (WI-38).

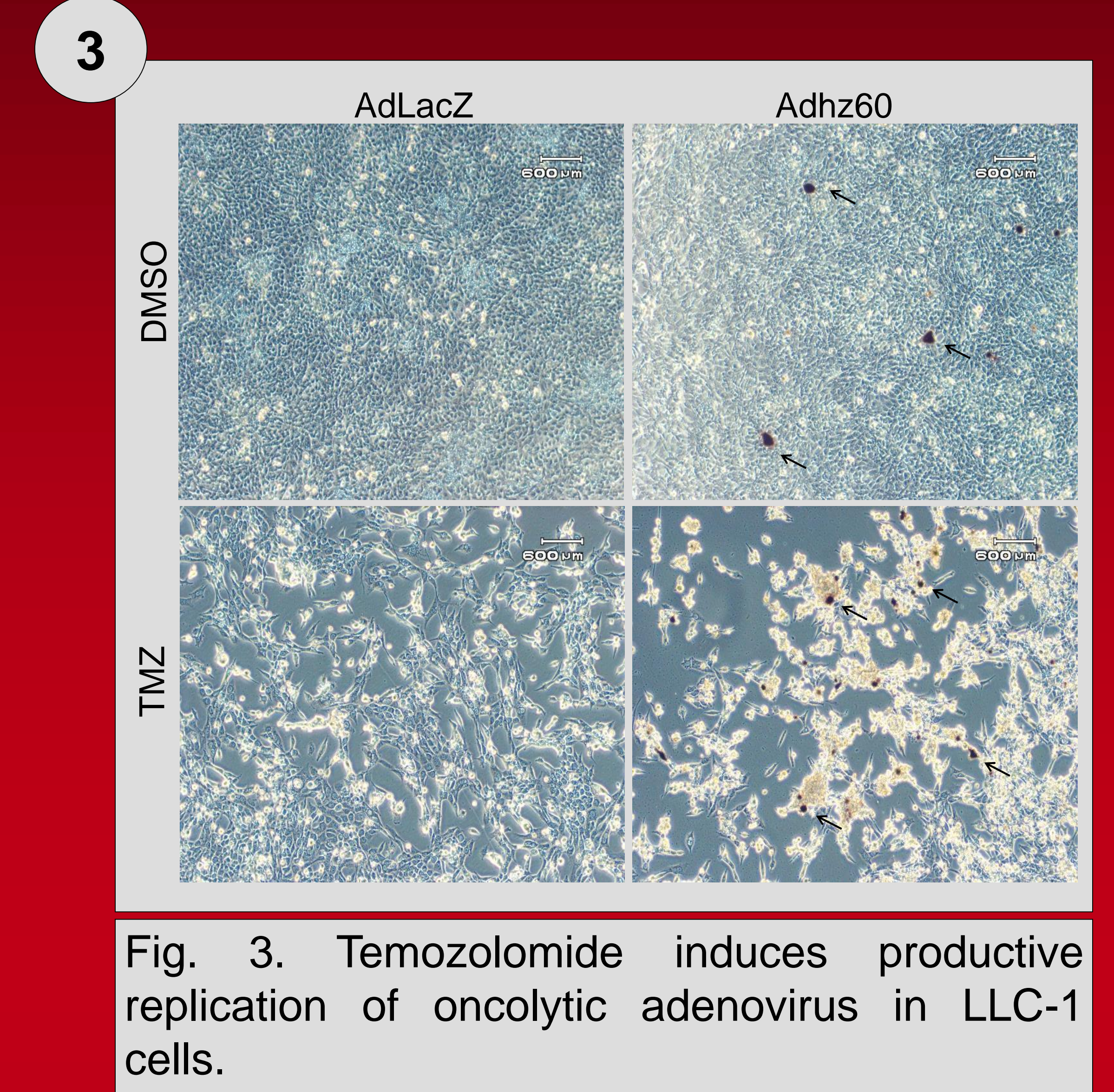


Fig. 3. Temozolomide induces productive replication of oncolytic adenovirus in LLC-1 cells.

## Conclusions

This study provides evidence that syngeneic mouse LLC-1 cells treated with TMZ became susceptible to human oncolytic Ad replication. Additionally, TMZ-induced autophagy might not be required for TMZ-enhanced oncolytic adenovirus replication.

In this study it was also found that the combination therapy of oncolytic adenovirus (Adhz60) with TMZ resulted in a synergistic cancer cell killing effect and apoptosis induction. Minimal cytotoxicity was observed in human lung normal cells.

This approach will provide an excellent model for a better understanding of interaction between the immune system and oncolytic adenovirus replication.

## Acknowledgements

Research supported by the School of Medicine Summer Research Scholar Program grant R25-CA-134283 from the National Cancer Institute (E.R.).



# Predicting adverse events in patients undergoing hepatectomy – validation of preoperative nomogram and risk score

Travis Spaulding, BS, Robert CG Martin II, MD, PhD

Department of Surgery, Division of Surgical Oncology, University of Louisville, Louisville, KY

## Introduction

Malignancy in the liver, including the biliary tree, has many etiologies, including hepatocellular carcinoma, metastatic cancer from primary colorectal or breast, cholangiocarcinoma, and gallbladder carcinoma. Management of these conditions is often accomplished at least in part through hepatectomy, with therapeutic options ranging from ablation, to wedge resection, to full lobectomy. It is important that physicians have the means to effectively quantify the risk of morbidity in patients preoperatively, for the benefit of the patient.

There is much published research on preoperative measures of postoperative mortality in the surgical treatment of liver malignancies, but little on morbidity. *Dhir et al.* and *Simons et al.* have a published preoperative nomogram and perioperative risk score, respectively, assessing the risk of mortality post-hepatectomy.

## Hypothesis and Aims

**Hypothesis:** Preoperative nomograms and perioperative risk scores for mortality in the surgical management of liver malignancy also have significant clinical utility in predicting morbidity.

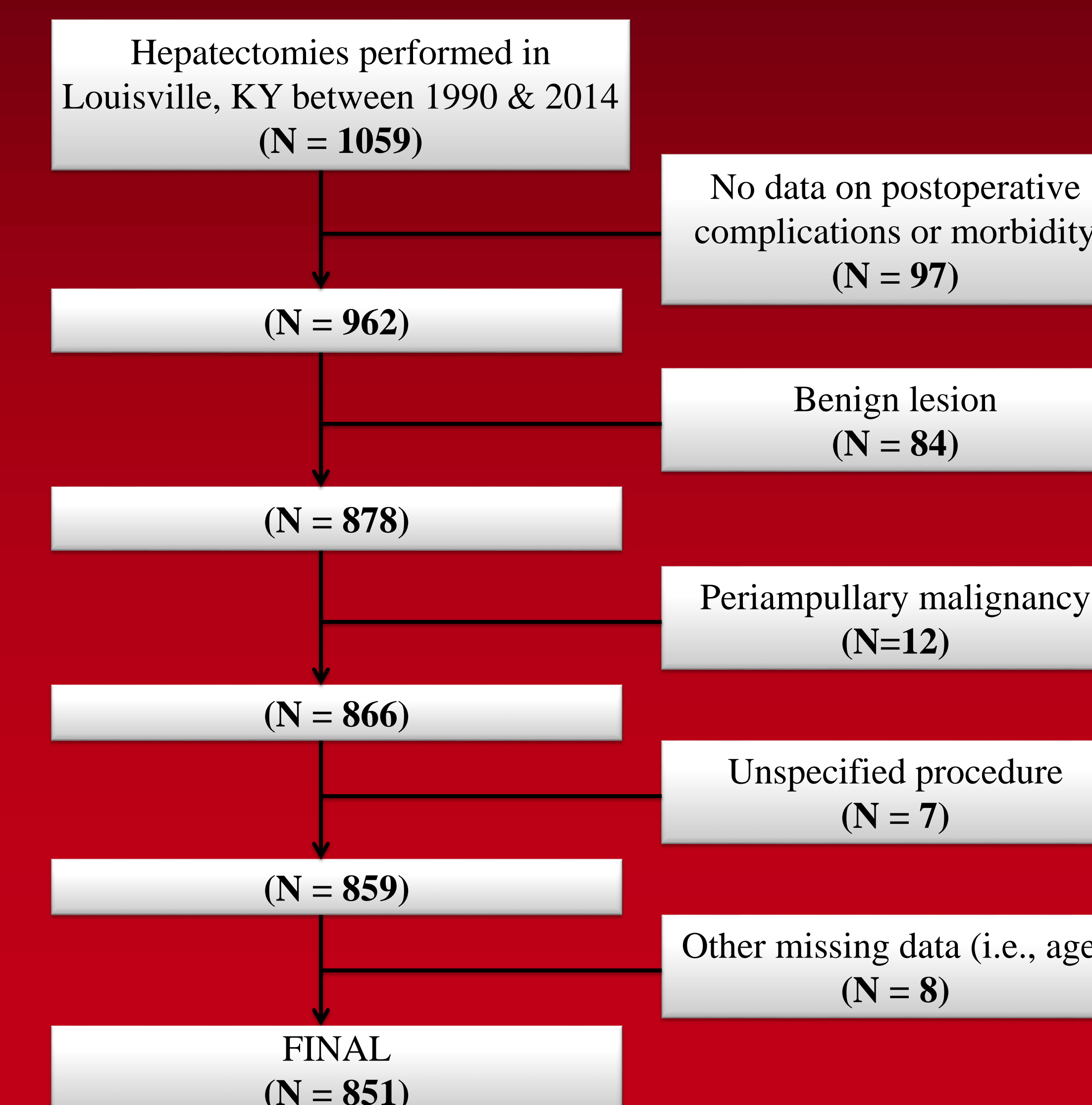
**Aims:**

- To validate the published calculations as acceptable measures of postoperative mortality following hepatectomy.
- To assess the value of these published measures in predicting postoperative morbidity following hepatectomy.

## Methods

- Data was collected from a prospectively managed dataset of 1059 hepatectomies performed in Louisville, Kentucky from December 20, 1990 to April 11, 2014. After patient exclusion (shown in Figure 1), 851 procedures were analyzed.
- Exclusion criteria included lack of data, management of benign lesions, or any periampullary malignancy.
- Preoperative data was used to assign scores for each published measure and the scores were sorted into clinically relevant groups with corresponding ordinal scores, according to the previously published literature.

Figure 1: Patient Selection Flow Diagram



## Results

- Both the *Dhir et al.* nomogram (p=0.0004) and *Simons et al.* risk score (p=0.0017) were acceptable predictors of postoperative mortality, confirming past research.
- In the analysis of morbidity, scores according to *Dhir et al.* were a poor predictor of morbidity.
- The ordinal risk score published by *Simons et al.* was predictive of complications (p=0.0029), the number of complications (p=0.0028), complication grade (p=0.0033), and hepatic-specific complications (p=0.0003).
- Type of incision was also a predictor of post-operative morbidity (p < 0.0001), although this is not a preoperative variable.

## Clinical Utility in Assessing Morbidity

Table 3. Components of the perioperative risk score as previously published by *Simons et al.*

Factor	Level	Point Value	
		Liver Metastases	Liver Primary
Age group	≤ 55	0	0
	56–64	1	1
	65–74	2	1
Charlson score	> 75	6	4
	0	0	0
	1	2	3
Procedure type	2	4	4
	≥ 3	10	8
	RFA/enucleation	3	2
Sex	Wedge resection	3	2
	Lobectomy	6	6
Hospital Type	Female	1	0
	Male	0	1
	Teaching	0	0
	Non-teaching	2	3

## Discussion

- Mortality was effectively predicted by the nomogram and risk score, validating published research, indicating that this study's sample and those of previous studies do not significantly vary in their surgical outcomes.
- For the *Simons et al.* risk score, values were not predictive of morbidity (or mortality) unless they were sorted into groups based on clinical likelihood of a mortality.
- Future directions:
  - Quantifying risk for postoperative morbidity based on easy-to-measure factors (smoking, drinking, etc.)
  - Discover role of incision in patient morbidity. Which favors better outcomes?

Tables 1 & 2: *Simons et al.* & *Dhir et al.* ordinal grouping data

<i>Simons, et al.</i> Risk Score Group	1 (R.S.: 1-4)	2 (R.S.: 5-9)	3 (R.S.: 10-14)	4 (R.S.: ≥ 15)
<b>N (patients)</b>	18	394	340	99
<b>N (complications)</b>	5	183	181	165
<b>(complications per patient)</b>	0.278	0.464	0.532	1.667
<b>Complications</b>				
Yes	6 (33.33%)	149 (37.82%)	152 (44.71%)	57 (57.58%)
No	12 (66.67%)	245 (62.18%)	188 (55.29%)	42 (42.42%)
<b>Incision</b>				
Hockey Stick	2 (11.11%)	84 (21.32%)	101 (29.71%)	22 (22.22%)
Midline	8 (44.44%)	90 (22.84%)	63 (18.53%)	23 (23.23%)
Subcostal	3 (16.67%)	107 (27.16%)	54 (15.88%)	19 (19.19%)
Laparoscopic	3 (16.67%)	67 (17.01%)	70 (20.59%)	18 (18.18%)
Mercedes/Chevron	0 (0.00%)	17 (4.31%)	38 (11.18%)	11 (11.11%)
Unknown	2 (11.11%)	29 (7.36%)	14 (4.12%)	6 (6.06%)
<b>Liver Procedure</b>				
Ablation/Enucleation	10 (55.56%)	205 (52.03%)	73 (21.47%)	19 (19.19%)
Caudate or Central Liver Resection	0 (0.00%)	24 (6.09%)	10 (2.94%)	1 (1.01%)
Atypical Resection	5 (27.78%)	17 (4.31%)	6 (1.76%)	0 (0.00%)
Left Lateral Segmentectomy	2 (11.11%)	58 (14.72%)	12 (3.53%)	3 (3.03%)
Right Posterior Sectomy	0 (0.00%)	23 (5.84%)	5 (1.47%)	1 (1.01%)
Lobectomy	1 (5.56%)	46 (11.68%)	154 (45.29%)	49 (49.49%)
Trisegmentectomy	0 (0.00%)	16 (4.06%)	59 (17.35%)	23 (23.23%)
Orthotopic transplantation	0 (0.00%)	5 (1.27%)	21 (6.18%)	3 (3.03%)
<b>Major/Minor</b>				
Major	1 (5.56%)	56 (14.21%)	186 (54.71%)	57 (57.58%)
Minor	17 (94.44%)	338 (85.79%)	154 (45.29%)	42 (42.42%)
Mean: BMI	26.25	27.71	27.37	27.67
Mean: Highest complication grade	2.50	2.46	2.79	2.80
Mean: Sum of complication grades	1.17	1.34	1.69	2.52

<i>Dhir, et al.</i> Nomogram Score Quartile	1st	2nd	3rd	4th
<b>N (patients)</b>	224	221	193	213
<b>Nomogram Score</b>				
Mean	87.58	118.85	138.57	179.75
Median	91	116	143	172
Range	29 – 99	109 – 124	126 – 150	151 – 271
<b>N (complications)</b>	98	118	98	121
<b>(complications per patient)</b>	0.438	0.534	0.508	0.568
<b>Complications</b>				
Yes	88 (39.29%)	95 (42.99%)	87 (45.08%)	93 (43.66%)
No	136 (60.71%)	126 (57.01%)	106 (54.92%)	120 (56.34%)
<b>Incision</b>				
Hockey Stick	45 (20.09%)	67 (30.32%)	45 (23.32%)	52 (24.41%)
Midline	53 (23.66%)	59 (26.70%)	39 (20.21%)	33 (15.49%)
Subcostal	56 (25.00%)	46 (20.81%)	39 (20.21%)	42 (19.72%)
Laparoscopic	38 (16.96%)	36 (16.29%)	34 (17.62%)	50 (23.47%)
Mercedes/Chevron	12 (5.36%)	8 (3.62%)	21 (10.88%)	25 (11.74%)
Unknown	20 (8.93%)	5 (2.26%)	15 (7.77%)	11 (5.16%)
<b>Liver Procedure</b>				
Ablation/Enucleation	108 (48.21%)	76 (34.39%)	68 (35.23%)	55 (25.82%)
Caudate or Central Liver Resection	12 (5.36%)	9 (4.07%)	12 (6.22%)	2 (0.94%)
Atypical Resection	15 (6.70%)	6 (2.71%)	6 (3.11%)	1 (0.47%)
Left Lateral Segmentectomy	37 (16.52%)	21 (9.50%)	11 (5.70%)	6 (2.82%)
Right Posterior Sectomy	10 (4.46%)	13 (5.88%)	3 (1.55%)	3 (1.41%)
Lobectomy	32 (14.29%)	72 (32.58%)	55 (28.50%)	91 (42.72%)
Trisegmentectomy	9 (4.02%)	24 (10.86%)	24 (12.44%)	41 (19.25%)
Orthotopic transplantation	1 (0.45%)	0 (0.00%)	14 (7.25%)	14 (6.57%)
<b>Major/Minor</b>				
Major	34 (15.18%)	77 (34.84%)	76 (39.38%)	113 (53.05%)
Minor	190 (84.82%)	144 (65.16%)	117 (60.62%)	100 (46.95%)
Mean: BMI	28.52	27.21	27.24	27.11
Mean: Highest complication grade	0.83	0.96	0.87	1.10
Mean: Sum of complication grades	1.38	1.70	1.45	1.92

## Acknowledgements

National Cancer Institute—Grant R25-CA134283

# Targeting cytosolic aspartate aminotransferase in human pancreatic and lung carcinoma using a novel inhibitor *in vitro*



Govind Warriar, Yoannis Imbert-Fernandez, Rob Spaulding, Jordan Noe, Brian Clem, John Trent, Jason Chesney



## Abstract

Increased glycolytic metabolism is a hallmark of neoplastic cells that allows self-promotion of growth and survival. The malate-aspartate shuttle (MAS) plays a significant role in optimizing energy output from glycolysis by facilitating the transfer of electrons from cytosolic NADH for use in mitochondrial electron transport. A key enzyme in the MAS pathway is aspartate aminotransferase (AAT/GOT1), of which there are cytosolic (cAAT) and mitochondrial (mAAT) variants. Recently, AAT has also been found to be integral in proliferation of human pancreatic ductal adenocarcinoma (PDAC) through its role in increasing the NADPH/NAD<sup>+</sup> ratio allowing maintenance of the cellular redox state (2). Studies show inhibition of AAT with aminooxyacetate (AOA), a known inhibitor of transaminases, decreases proliferation of PDAC and breast adenocarcinoma cells (1).

Based on the overexpression of AAT in carcinoma containing Ras oncogene mutations, along with the critical role of AAT in the aforementioned metabolic pathways, we hypothesize that AAT may be a suitable target for future cancer therapeutics. Through an active site binding screen of cAAT, novel inhibitors 117 and 4-47 were discovered. 117 and 4-47 were both found to decrease cell growth in pancreatic adenocarcinoma, alveolar adenocarcinoma, and large cell lung cancer, in tissue culture. Treatment with 4-47, in particular, displayed drastic reductions in growth. An *in vitro* AAT assay revealed inhibition of cAAT activity by 4-47. These findings demonstrate 4-47 to be an inhibitor of cAAT warranting further investigation as a potential therapeutic.

## Methods

### In-vitro AAT Activity Assay

- AAT activity was measured in the presence of various concentrations (1μM, 10μM, 25μM) of 4-47. The assay mix contained L-aspartate (2mM, 10mM, 20mM, or 100mM), 120mM α-ketoglutarate, Malate DH, and 1mg/mL NADH in 50mM Tris buffer. Whole cell lysate of H460 cells was then added to the reaction mixture and the decrease in absorbance at 340nm was measured using a 96-well plate reader with a kinetics protocol.

### Cell Viability Assay

- MiaPaca2, A549, and H460 cells were plated in a 24-well plate at a density of 20,000 cells/well. Cells were treated with DMSO vehicle control or 1μM, 5μM, 10μM, 30μM, 50μM, 100μM of 117 or 4-47. 48 hours after treatment, viable cells were counted.

## Background

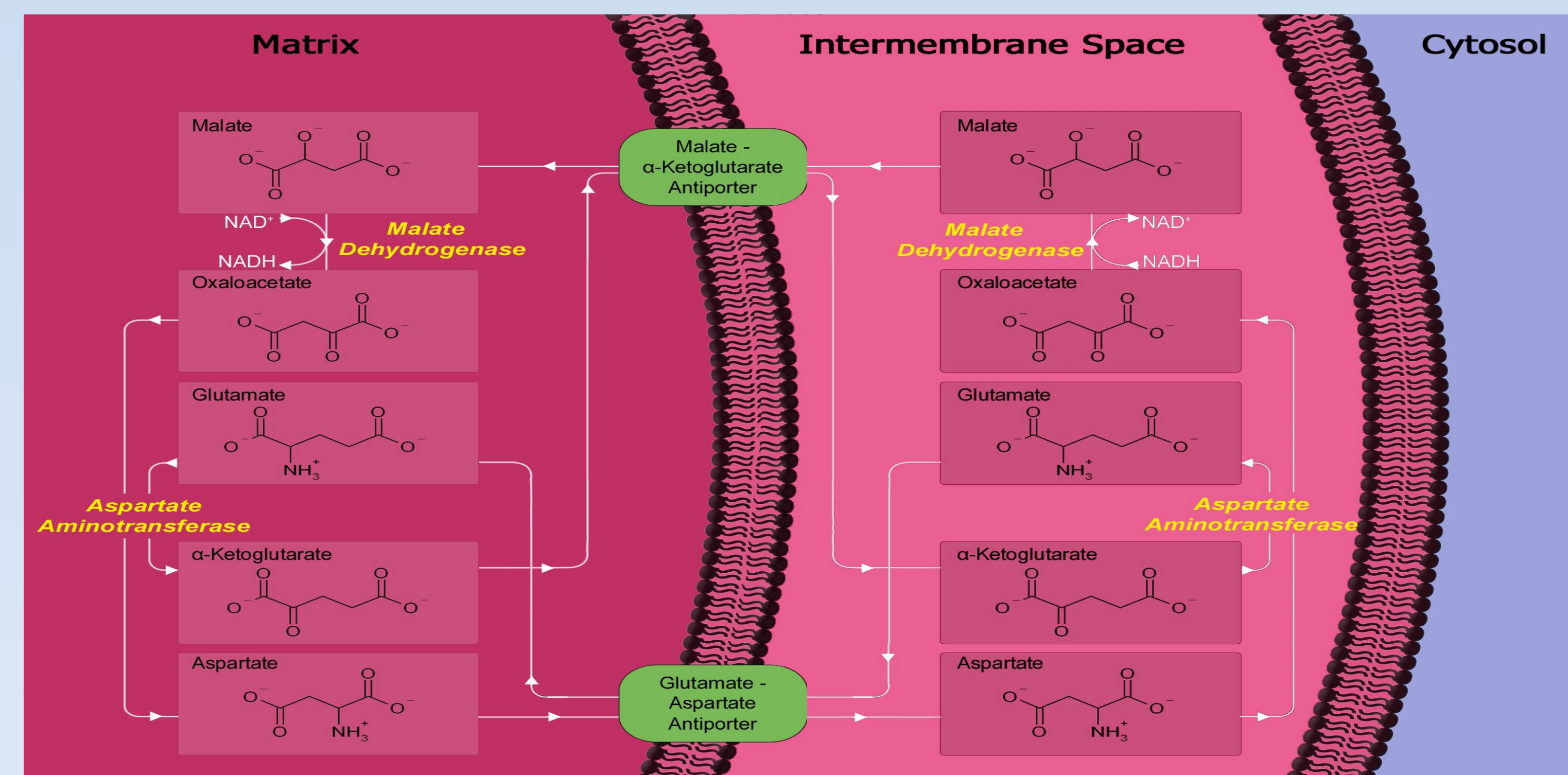


Figure 1: Malate-Aspartate Shuttle

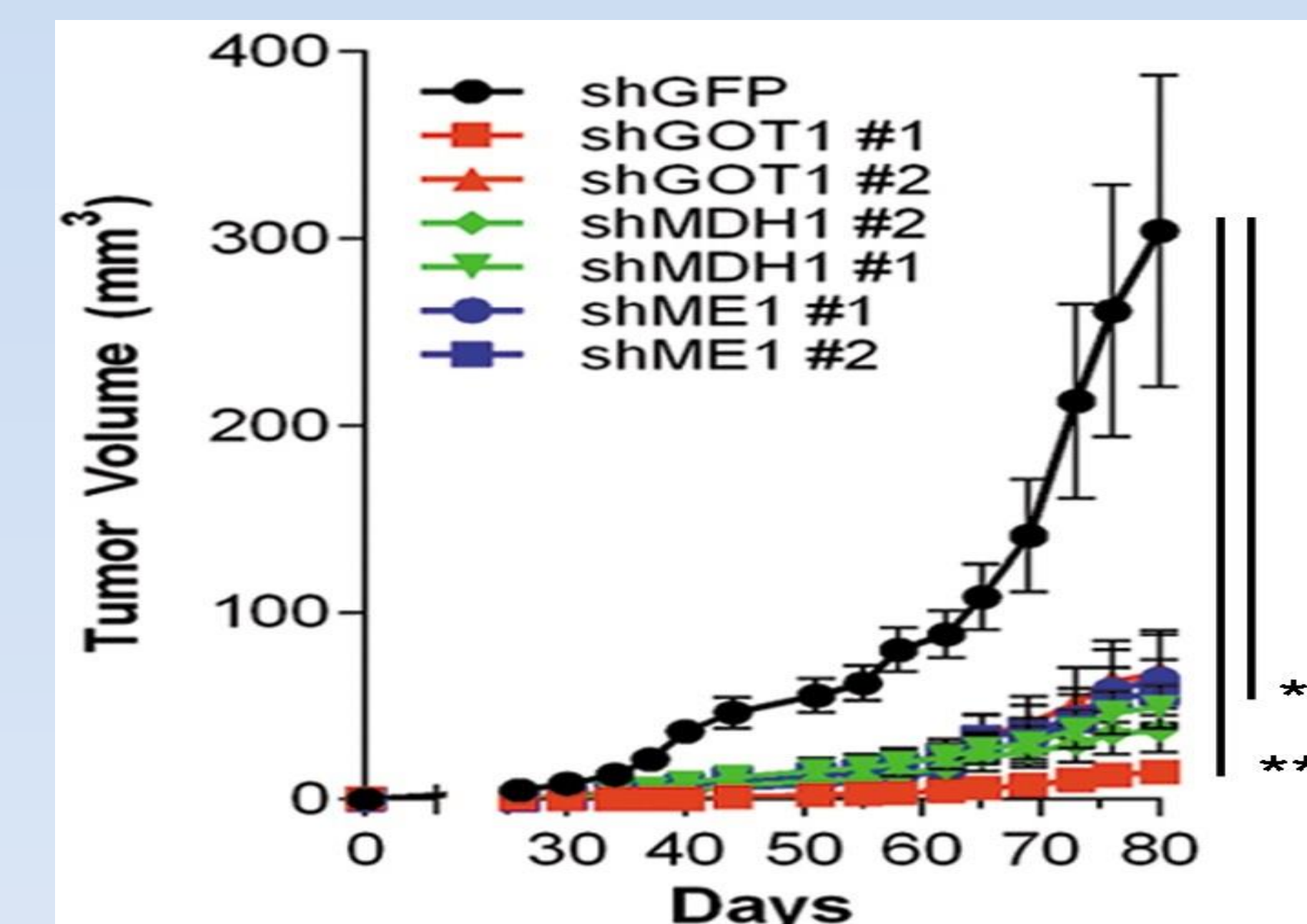


Figure 2: shRNA inhibition of Malate-Aspartate Shuttle Enzymes on xenograft growth of 8988T cells (2)

## Conclusions

- Growth of human pancreatic adenocarcinoma, alveolar adenocarcinoma, and large cell lung cancer were reduced by treatment with drugs 117 and 4-47, *in vitro*
- Treatment with 4-47 showed an especially drastic decrease in cell proliferation and AAT activity assay revealed some specificity for AAT enzyme
- Findings warrant further investigation into 4-47 as a potential inhibitor of AAT

## Results

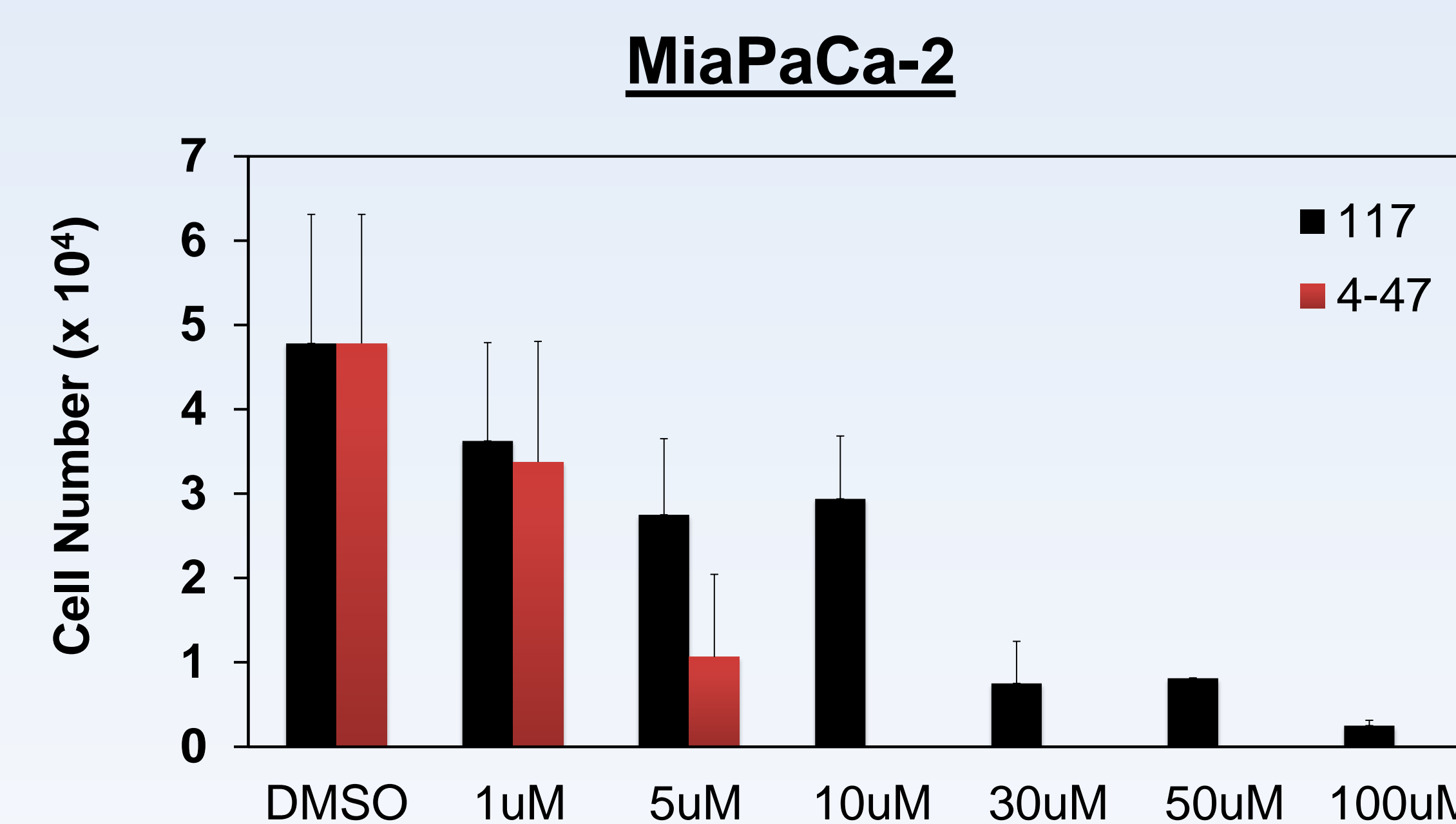


Figure 3: MIAPaCa-2 inhibition by 48h treatment with various concentrations of 117 and 4-47

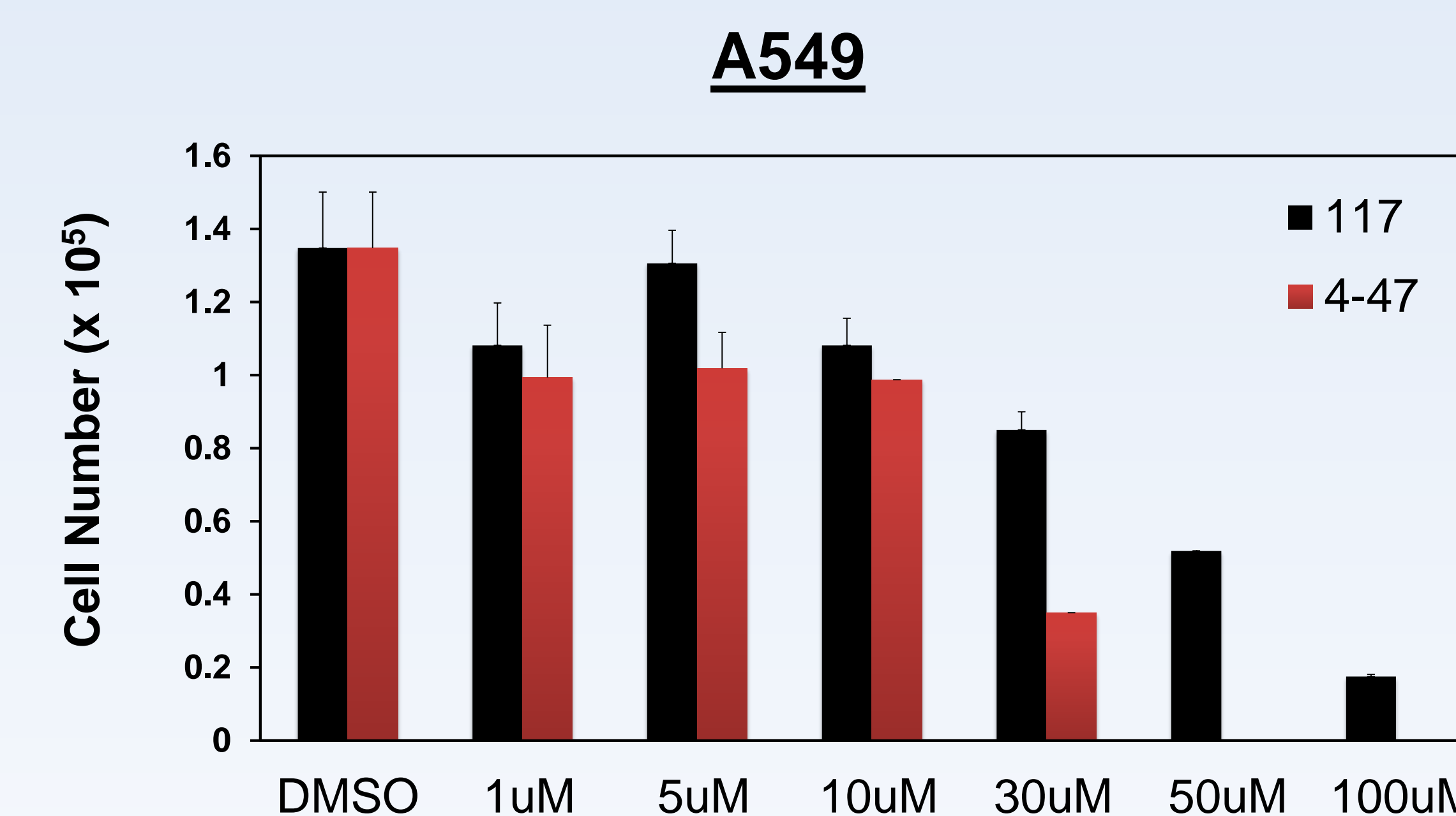


Figure 4: A549 inhibition by 48h treatment with various concentrations of 117 and 4-47

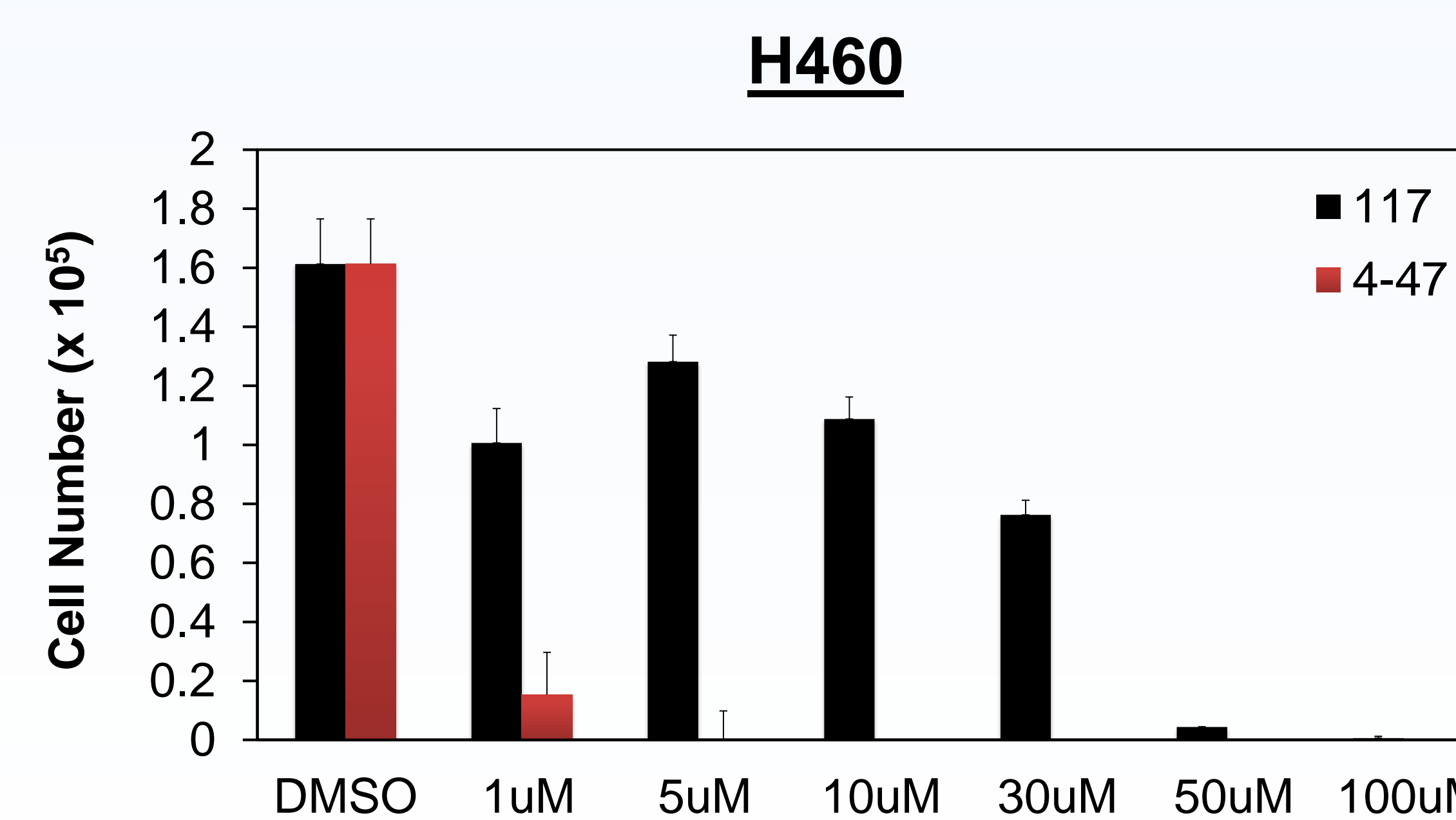


Figure 5: H460 inhibition by 48h treatment with various concentrations of 117 and 4-47

### 4-47 Inhibition of AAT in H460 Cells

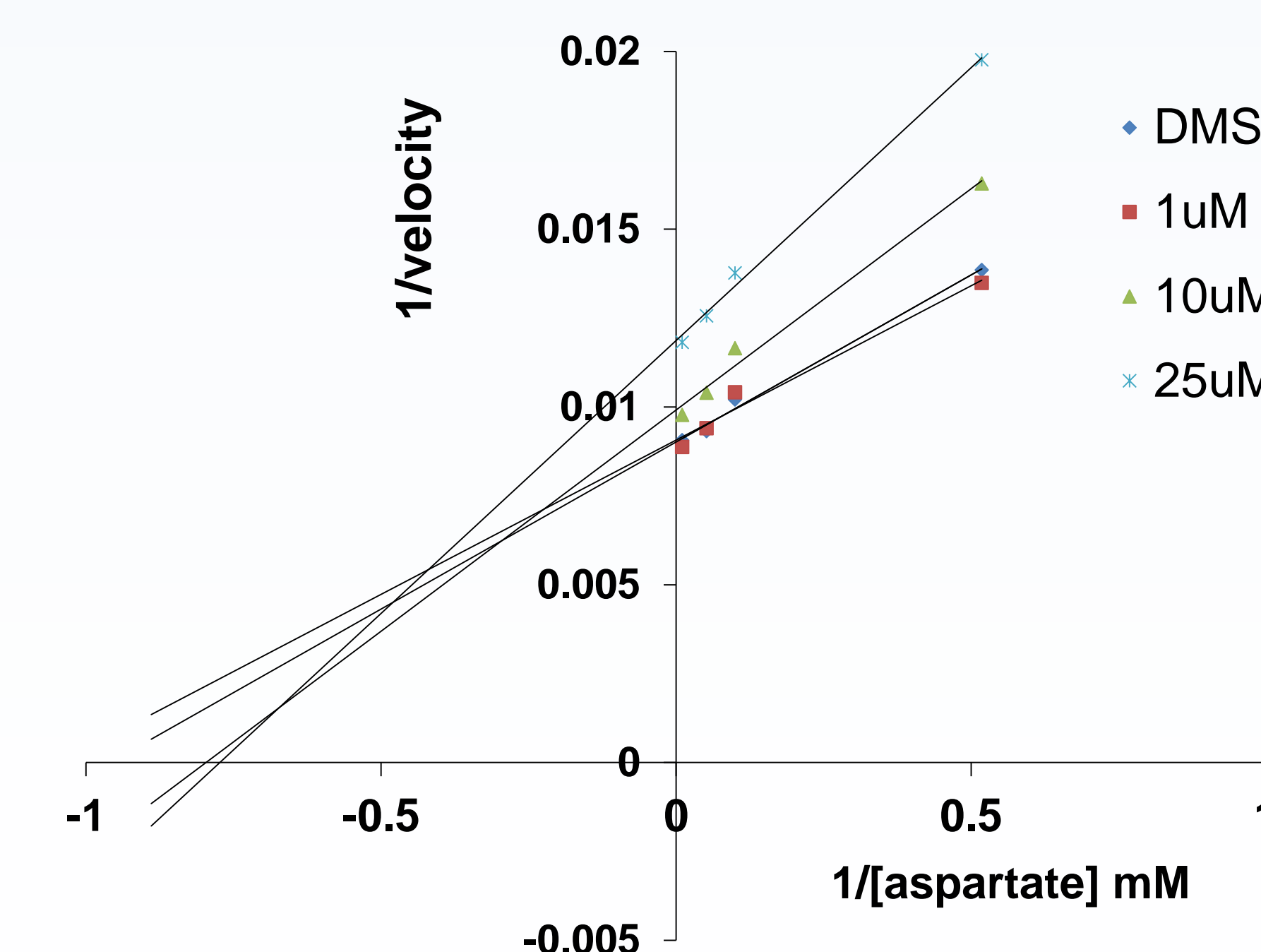


Figure 6: Lineweaver-Burke plot of AAT inhibition in H460 whole cell lysate by 4-47

## Future Studies

- Cell viability assay in Panc-1 cell line
- In-vitro* AAT activity assay in MiaPaCa-2, A549, and H460 cell lines
- Pure *in vitro* AAT activity assay

## References

- Thornburg JM, Nelson KK, Clem BF, Lane AN, Arumugam S, Simmons A, Eaton JW, Telang S, Chesney J. Targeting aspartate aminotransferase in breast cancer. 2008;10(5)
- Son J, Lyssiotis CA, Ying H, Wang, X, Hua S, Ligorio, M, Perera RM, Ferrone CR, Mullarky E, Shyh-Chang N, Fleming JB, Bardeesy N, Asara JM, Haigis MC, DePinho RA, Cantley LC, Kimmelman AC. Glutamine supports pancreatic cancer growth through a KRAS-regulated metabolic pathway. Nature 2013; 499(7459)

## Acknowledgements

Research supported by the NIH/NCI R25-CA-134283 grant and the University of Louisville Cancer Education Program

# Expression and Analysis of GST-tagged UBR5 Protein

Dexter Weeks, Kumar. Saurabh, Ph.D, Levi J. Beverly, Ph.D.

Department of Medicine, James Graham Brown Cancer Center  
University of Louisville School of Medicine, Louisville, KY 40202

## Abstract

Investigation of ubiquitination and proteasome degradation pathways is essential to the field of cancer biology and therapeutics because of their role in cellular proliferation and apoptosis. Of particular interest is the targeting of UBR5 due to its potential role in solid tumor formation. Our previous data demonstrate that siRNA mediated loss of UBR5 is detrimental to lung cancer cell survival. Our objective in this study was to induce bacterial cultures to express and purify the UBR-box of UBR5 proteins. We hypothesize that knockout of UBR5 provides chemotherapeutic benefit in mouse models for lung cancer. Subsequently, the findings of this process would allow for future investigation into the biochemical mechanisms by which putative inhibitors of UBR5 act.

## Background

Nearly 40% of cancers that include cervical, lung, breast, bladder, and ovarian carcinoma are linked to copy number variations or mutation in UBR-box genes. Study of the UBR-box genes is crucial to developing better prognoses and therapeutic approaches for cancer patients. Our prior data shows mutated or amplified UBR5 in human lung adenocarcinoma as well as other cancers. Our study of the UBR-box is especially concerned with the N-end rule ubiquitination pathway and if it plays a causal role in tumorigenesis. As reported by the National Cancer Institute, lung cancer has worldwide predominance as the leading cause of cancer mortality. The impact of further investigation to UBR5 entails greater understanding of the ubiquitin-proteasome degradation pathway as it relates to tumor suppression and oncogenic regulation.

To this end, using mouse models have proven instrumental in investigating the biologic effects of UBR5 knockout. Prior findings have shown the capability for siRNA- and shRNA-mediated loss of UBR5. Through further inquiry, there is also focus on viability of systemic UBR5 knockdown. Purifying UBR5 will allow for characterizing its interaction with substrate proteins to assess if this form of cytotoxic cancer therapy is an efficacious option for lung adenocarcinoma.

## Methods

### Induction

Cultures of recombinant E. coli were induced to express GST using the pGEX GST expression vector during bacterial transformation. The three cultures were respectively transformed to express GST, GST-tagged UBR-box with 35 amino acid of flanking sequences, and GST-tagged UBR-box with 100 amino acid of flanking sequences. Addition of flanking sequences to the protein increased the chances of obtaining a properly folding protein. After transformation, the bacteria were induced to express the proteins via introduction of 0.1 millimolar IPTG reagent.

### Lysis

Each respective E. coli culture underwent lysis through administration of lysis buffer and subsequent sonication.

### Western Blot analysis

Initially, the entirety of each bacterial lysate was analyzed via Western blot to confirm the expression of UBR-box. Afterwards, analysis of the soluble fraction from each culture was analyzed for presence of the desired protein.

## Conclusions

The findings revealed the E. coli cultures expressed their desired GST-tagged proteins, however only the GST-only culture produced protein found in the soluble fraction after lysis. Since GST is known to improve the solubility of proteins, we must reassess the flanking sequences or lysis methods to assure proper folding and solubility for peptide pull-down.

Since UBR5 has been proven to be overexpressed in approximately 40% of human cancers, experimentation on properly purified UBR5 protein will uncover the benefits of UBR5-specific inhibition as a cytotoxic therapeutic approach for lung cancer.

## Future Directions

Peptide pull-downs with immobilized peptides known to bind to UBR-box and identify which compounds block the peptide/UBR5 interaction

Treating cells with UBR5 inhibitor compounds to look for loss of protein interactions

Inhibition of UBR5 in inducible shRNA mouse model and determine *in vivo* outcomes

Determine if systemic UBR5 loss is tolerable and if UBR5 loss exhibits a therapeutic benefit following cytotoxic treatment of lung cancer mouse models of cancer.

## Acknowledgements

Research supported by grant R25-CA-134283 from the National Cancer Institute.

Many thanks to the members of the Beverly lab for assistance and guidance, with special thanks to Dr. Kumar Saurabh and Dr. Levi Beverly for their instruction and mentorship.

## Results

### Western Blot analysis of UBR-box with recombinant protein tags



Figure 1. Western blot showing expression of UBR-box proteins with GST tags from IPTG-induced E. coli

Figure 2. Western blot showing soluble fraction of UBR-box proteins with GST expressed by induced E. coli